Low- and high-pressure *ab initio* equations of state for the alkali chlorides

J. M. Recio, A. Martín Pendás, E. Francisco, M. Flórez, and Víctor Luaña
Departamento de Química Física y Analítica, Facultad de Química,
Universidad de Oviedo, 33006 Oviedo, Spain
(Received 15 April 1993)

We have carried out *ab initio* perturbed ion calculations in the rocksalt (B1) and cesium chloride (B2) phases of the alkali (A) chloride (ACl) crystals. Zero temperature (T), and pressure (P) lattice energies and equilibrium distances are computed with errors less than 5%. From static calculations, zero-T equations of state (EOS) are reported in the ranges of 0–80 GPa for LiCl, 0–60 GPa for NaCl and KCl, 0–10 GPa for RbCl, and 0–5 GPa for CsCl. Since experimental data are a critical test of the performance of a theoretical methodology, we have placed particular emphasis on (a) the comparison between calculated and experimental trends and (b) the consistency with the behavior observed in real materials. We have found that our theoretically modeled solids obey the Vinet *universal* EOS and match the experimental behavior in temperature-scaled EOS diagrams. We have also analyzed the phase stability of the ACl crystals from a thermodynamic point of view. The hydrostatic pressure neccessary to produce the B1-B2 phase transition is calculated to decrease with the cation size, in agreement with the experimental observation. Our predicted value of the (not yet measured) B1-B2 transition pressure for LiCl is close to 80 GPa. Finally, our calculations based on the combined kinetic-thermodynamic model proposed by Li and Jeanloz for the NaCl transition phase [Phys. Rev. B **36**, 474 (1987)] predict that the hysteresis pressure range of the B1-B2 transition decreases from LiCl to RbCl.

I. INTRODUCTION

The determination of the pressure-volume-temperature (P-V-T) relation of solid materials is a problem of considerable importance in basic and applied science.[1] Much effort towards reliable simulation of condensed-matter equations of state (EOS) has been and is currently being expended in phenomenological (PH) and quantum-mechanical (QM) modeling. PH models describe the total energy of solids in terms of interactions between their atomic (ionic) components, and may or may not include many-body contributions. These interactions are modeled by analytical expressions that may be obtained from experimental data or calculated from first principles. On the other hand, QM simulations try to solve the Schrödinger equation of the solid using some feasible methodology.

Ionic crystals are among the solids on which PH calculations have been more extensively performed. The basic strategy in using empirically derived pairwise potentials is described in the classic text of Born and Huang[2] and in the review by Tosi.[3] Some of the results for the alkali halides, recently analyzed by Khwaja *et al.*,[4] correctly predict the stable phase at zero P, T, but give unrealistic trends in the transition properties from the rocksalt (B1) to the cesium chloride (B2) structure. Recently, very elaborate semiempirical PH calculations, based on the three-body interatomic potentials of Jog, Singh, and Sanyal,[5] have been performed by Prabhakar *et al.*[6] on NaCl and KCl and by Rao and Sanyal[7] on sodium halides. Their results reproduce accurately the experimental transition phase data.

The main source of first-principles PH simulations is the electron-gas theory of Gordon and Kim (GK).[8] A number of these calculations incorporating refinements of the initial version of the model have been carried out. One of the modifications includes the use of pseudocrystalline wave functions, depending on lattice parameters, as input to the GK model. This is the basis for the potential-induced-breathing (PIB) model.[9] Within GK theory, Boyer[10] calculated the EOS of 16 halides and concluded that the pair-potential approximation is in great need of improvement. Later, Feldman *et al.*[11] analyzed the Decker EOS (Ref. 12) for NaCl with GK models including PIB. Their results progressively differ from experiments as the pressure increases. Recently, Zhang and Bukowinski,[13] using a modified PIB model, have obtained good agreement with respect to the experimental EOS and B1-B2 transition data of several binary chlorides and oxides.

Alkali halides have also been used as a test bed for quantum-mechanical methodologies,[14–16] although few calculations of EOS and phase stability have been reported for them. The exception is the extensive work of Löwdin[14] based on the Hartree-Fock approach. More recently, Yamashita and Asano,[17] using standard Korringa-Kohn-Rostocker band calculations within the local-density approximation (LDA),[18] have studied several alkali halides and alkaline-earth chalcogenides. They found correct predictions of lattice energy and EOS but incorrect predictions of the stable phases for NaF, KCl, and CaS, even at atmospheric pressure. Froyen

and Cohen[19] have investigated the structural behavior of NaCl and KCl under high pressure using an LDA-pseudopotential method. Their results are in agreement with room-temperature experimental data for NaCl, but some discrepancies appear in the B2 phase of KCl due to an overestimated value of the bulk modulus. Feldman, Mehl, and Krakauer[20] have criticized these results, and especially the good prediction of the transition pressure in NaCl, and have concluded that extra energetic contributions beyond the LDA are needed to improve the agreement between theory and experiment.

From the experimental side, the situation also calls for a systematic investigation of the ACl EOS. Although P-V-T data and EOS of the B1 low-pressure structures are in general well established, it is also remarkable that high-pressure and, specially, transition phase data are affected by experimental uncertainties and nonhydrostatic effects.[19(a)] As an example, Li and Jeanloz[21] have recently observed the pressure-induced B1-B2 transition in NaCl. They have reported that there exists a significant hysteresis of about 7 GPa at room temperature, being 26.6±0.5 GPa the estimated thermodynamic transition pressure. This picture contrasts with the small hysteresis of the phase transformation pointed out by Basset *et al.*[22] and the value of 30 GPa assumed as the thermodynamic phase boundary for the NaCl B1-B2 transition.

Moreover, the more recent sets of isothermal P-V data for NaCl (Ref. 23) and KCl (Ref. 24), extending up to 70 and 56 GPa, respectively, are highly demanding tests for the QM model to be used. We also note that the lack of experimental information about the phase transition on the LiCl crystal adds an extra motive to the theoretical simulation of the ACl family.

In this paper, we apply the *ab initio* perturbed ion (AIPI) method[16] to extensively research the zero-temperature behavior of alkali chlorides (ACl) from the low to the high range of pressures. Our basic purpose is threefold: (a) to simulate the behavior of ACl crystals in a wide range of P-V conditions by means of a quantum-mechanical methodology, (b) to establish procedures to compare 0-K theoretical results with available experimental data, and (c) to predict values and trends of properties not yet measured in the laboratory. In addition, AIPI calculations can (a) supply crystal data for experimentally unstable states, (b) give a detailed quantum-mechanical analysis of the ACl crystalline EOS. However, in the following we will exclusively concentrate in macroscopic-thermodynamic aspects, whereas the microscopic-quantum examination, currently in progress, will be the subject of a subsequent publication.[25]

In the AIPI method, the multielectronic and many-body problem of the crystal is simplified within the theory of electronic separability[26] formalism by a double self-consistent requirement in the monocentric wave functions of each different ion of the crystal. The first requirement is the usual consistency between monoelectronic wave functions in the sense of the Hartree-Fock-Roothaan (HFR) approach. The second one stands for consistency with the crystalline environment in which the ion is embedded. The AIPI method provides this double consistency by solving iteratively the HFR equations of each ion interacting with the crystal potential created by the rest of the lattice.

The AIPI method has been successfully applied to the calculation of cohesive properties of closed-shell systems ranging from alkali hydrides and halides to rare-gas crystals. A compilation of results and a detailed description of the model has been given elsewhere.[27,28] Recently, the AIPI method has been used to predict the crystal response to high pressures in the rocksalt crystalline phase of ZnO and ZnS.[29] The last results were able to resolve the large discrepancies found between two different empirical EOS that had been used to extrapolate to zero-pressure P-V measurements on the high-pressure phase of ZnS.

In line with our previous work, we will emphasize here that to set up a benchmark of the ability of a QM methodolology, it is more convenient to show consistency between the theoretical and the experimental behavior on a whole set of properties than attaining quantitative agreement in some selected ones. What we mean by consistency is that the general behavior of the modeled solid follows the same empirical rules observed in real crystals. Providing such consistency, the QM model can be confidently applied in a predictive manner for other systems with limited available data. In order to test this consistency, we will analyze in this paper the AIPI results for the ACl crystals in four types of EOS: (a) the usual $V/V_0 - P$ isothermal relationship, (b) the temperature-scaled diagram recently proposed by Thakur and Dwary[30] to fit NaCl data in a wide range of temperatures, (c) the *universal* EOS form due to Vinet *et al.*,[31] and (d) the strain-stress curve.

The rest of the paper is organized as follows. In Sec. II, we briefly describe our computational scheme for total-energy and zero-T EOS calculations. In Sec. III, we present and discuss our results, and it is divided into three subsections. Analysis of the zero-P,T cohesive properties of B1 and B2 phases is carried out first; the EOS is then discussed in the four different forms indicated above; finally the relative stability of the B1-B2 phases is addressed. The paper ends with the main conclusions of our investigation in Sec. IV.

II. COMPUTATIONAL SCHEME

We introduce here some of the basic magnitudes of the AIPI model along with some technical details of the calculations presented in this work. A further description of the model can be found in Refs. 16 and 28.

A. Total energy

The main outcomes of any solid-state QM method are the wave function and the total energy of the crystal. The AIPI crystal wave function is an antisymmetrized product of monocentric ionic local functions. The local functions minimize the effective energies of the corresponding ion in the field of the crystal lattice. The effective energy

is written as a sum of the net or self-energy of the ion in the crystal and the ion-lattice interaction energy. Once the crystalline wave functions of the ions are obtained, the total energy is readily expressed as a sum of a monocentric term, involving net energies, and a bicentric contribution coming from the interaction between ions.[16,28] In the calculations presented here, we have added to the net energy a correlation energy correction following the Coulomb-Hartree-Fock (CHF) prescription proposed by Clementi and reviewed by Chakravorty and Clementi.[32]

For any crystal geometry, the lattice energy per molecule, $E_{\rm latt}$, is immediately obtained as the difference between the total energy and that of the isolated ions. The cohesive properties and elastic constants are generated from the values of the lattice energy at different geometries.

We have computed total static energies of ACl crystals (A =Li^+, Na^+, K^+, and Rb^+) for a wide set of values of the lattice parameter a, ranging from 6 to 15 bohrs in the B1 structure and from 3.46410 to 8.66025 bohrs in the B2 one. We have also computed total-energy values of CsCl in the B1 and B2 structures. Our results in this crystal must be handled carefully due to their lack of relativistic contributions and dynamical correlation (DC). These effects grow with pressure. For CsCl, we believe that the safe range of a should be reduced to 11.1–14.6 bohrs (B1) and 6.5–8.5 bohrs (B2).

In all the computations, we have used the multi-ζ Slater-type-orbital (STO) basis sets of Clementi and Roetti[33] for the initial description of the ions of the five ACl crystals. Quantum interactions are explicitly taken into account between each ion and all those belonging up to the tenth shell surrounding it. A shell is defined as the set of crystallographic-equivalent ions located at the same distance from a given ion. Beyond these shells, quantum effects are negligible. We have found some convergence problems only at few values of a, in the short-range regime. These points have been eliminated in order to avoid artificial effects at high-pressure calculations.

B. Zero-temperature equation of state

The static zero-T EOS is generated from the pairs $(E_{\rm latt}, a)$ using a simple two-step procedure. First, we fit a polynomial in a to the set of calculated points. Second, we determine the pressure P and the bulk modulus B at different molar volumes V by means of the following thermodynamic equations:

$$P = -\left(\frac{dE_{\rm latt}}{da}\right)\left(\frac{da}{dV}\right), \tag{1}$$

$$B = V\left[\left(\frac{d^2E_{\rm latt}}{da^2}\right)\left(\frac{da}{dV}\right)^2 + \left(\frac{dE_{\rm latt}}{da}\right)\left(\frac{d^2a}{dV^2}\right)\right]. \tag{2}$$

From Eq. (1), we obtain the static pressure contribution to P at 0 K. Cowley, Gong, and Hortan[34] have recently shown that the zero-point pressure $P_{\rm ZP}$ modifies only very slightly the zero-T EOS of NaCl. The minor role of $P_{\rm ZP}$ in the predictions of EOS and transition-phase data in the ACl crystals has been also discussed in other PH (Ref. 35) and QM (Ref. 19) calculations.

We have calculated P and B in a range of V according to the lattice parameters specified above for the B1 and B2 phases of the ACl crystals. The theoretical reported EOS cover the experimental high-pressure data in the ACl, except for the region from 60 to 70 GPa in NaCl, and for the problematic CsCl case. For this crystal we will only present some numerical results. The LiCl EOS is extended up to 80 GPa because it is near this region that we find the transition to the B2 phase, as we will see in the next section.

III. RESULTS AND DISCUSSION

A. Cohesive properties at zero T, P

The $E_{\rm latt}$ versus $R(A\text{-Cl})$ curves are plotted in Fig. 1 for the LiCl, NaCl, KCl, and RbCl crystals. The corresponding curves for CsCl have not been included in Fig. 1 for clarity. Some of the most interesting points emerging from this figure are the following.

(a) The B1 phase is the most stable structure at zero P, T for the four crystals, in agreement with the experimental observation.

(b) The computed values for the lattice energy $E_{\rm latt}$, the nearest cation-chloride equilibrium distance R_0, and the zero-pressure bulk modulus B_0, in the B1 phase follow the trend experimentally found for these crystals; namely, $-E_{\rm latt}$ decreases, R_0 increases, and B_0 decreases with the cation size. Our results predict the same trends for the experimentally unaccessible B2 structures. Numerical results are given in Table I and will be discussed

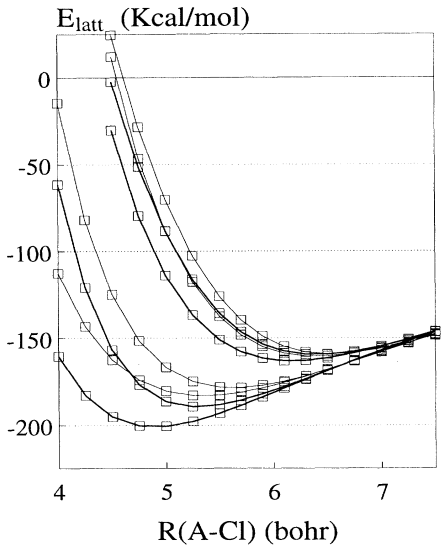

FIG. 1. Lattice energy of alkali halides. Thick and thin curves stand for B1 and B2 structures in the order (down to up) LiCl, NaCl, KCl, and RbCl. Symbols represent computed *AIPI* values.

TABLE I. Cohesive properties of alkali chlorides. First row: B1 calculations. Second row: B2 calculations. Third row: experimental values at 4.2 K or extrapolated data to 0 K, except numbers in brackets at 298 K.

		LiCl	NaCl	KCl	RbCl	CsCl
R_0 (Å)	B1	2.591	2.800	3.267	3.391	3.366
	B2	2.828	2.975	3.385	3.459	3.407
	Expt.	2.539[a]	2.789[a]	3.116[a]	3.259[a]	(3.571[b])
E_{latt}	B1	-200.8	-189.6	-163.1	-159.5	-161.0
(kcal/mol)	B2	-183.1	-178.8	-160.5	-159.2	-166.0
	Expt.	-202[c]	-185[c]	-170[c]	(-162[c])	(-155.1[d])
B_0 (GPa)	B1	31.2	28.8	15.5	15.3	10.0
	B2	24.1	25.6	19.6	19.3	12.5
	Expt.	35.5[e]	28.5[e]	20.2[e]	18.5[e]	(16.6[f])

[a]Ref. 39.
[b]Ref. 40.
[c]Ref. 41(a).
[d]Ref. 41(b).
[e]Ref. 35.
[f]Ref. 38.

further below.

(c) R_0(B1) is less than R_0(B2) in these ACl crystals. The zero-T, P stabilization energy $E_{\text{latt}}(\text{B2}) - E_{\text{latt}}(\text{B1})$ increases in passing from RbCl to LiCl, which is consistent with the observed greater B1-B2 transition pressure in the same sequence. For CsCl, the more stable phase at zero T, P is predicted to be the B2 structure (see Table I). These results also agree with other semiempirical and first-principles PH calculations.[7,35]

The zero-T, P properties for the B1 and B2 phases are collected along with experimental data in Table I, including results for CsCl. The overall comparison with our predictions is very satisfactory. R_0 and E_{latt} are predicted with errors less than 5%. The changes of these properties with the cation size broadly follow the experimental trends.

Comparisons between theoretical and experimental values of the equilibrium bulk modulus B_0 must be done with some care. On the one hand, B_0 is very sensitive to the details of the analytical fitting of $E_{\text{latt}}(a)$. An accurate estimation of B_0 needs many theoretical points of E_{latt} to be computed around a_0. On the other hand, B_0 increases quickly as the temperature decreases.[36,37] As Cohen and Gordon[35] have pointed out, static lattice values of B_0 should be compared with 0-K extrapolated values from experimental high-temperature data ($T > \Theta_D$), Θ_D being the Debye temperature. These authors reported such extrapolated values for the sodium, potassium, and rubidium chlorides, and the 4.2-K value for LiCl. We have included these numbers in Table I along with the value quoted by Li-Rong and Qing-Hu[38] for CsCl from their Vinet EOS fitting.

Once more, theoretical and experimental values follow the same trends, although, in this case, discrepancies as great as 25% appear. Errors are larger for heavier crystals, and this may be seen as a consequence of the lack of DC effects in the calculations. The DC takes into account correlation energy between electrons in different ions. Therefore, the DC should increase with the size of the cation, and it could be more important as the distance decreases. In principle, this effect would modify R_0, E_{latt}, and B_0 in the right direction in KCl and RbCl. For CsCl, we suspect that relativistic effects may play a significant role.

As a general behavior, Table I shows that the theoretical difference $B_0(\text{B1}) - B_0(\text{B2})$ decreases continuously with the cation size. Our predictions show that B_0 is larger in the B1 phase for LiCl and NaCl but smaller in the same structure for the potassium, rubidium, and cesium chlorides. These results give valuable information about the dissimilarities found in the response to pressure of each ACl crystal, and will be used later.

B. EOS diagrams

By means of Eqs. (1) and (2), we have plotted V/V_0-P and B-P curves for LiCl, NaCl, KCl, and RbCl in Fig. 2, V_0 being the corresponding computed zero-pressure volume of the B1 phase. Both kind of plots contain the same information. We will first consider the B1 results. Our computed B(B1) curves are continuously increasing functions of P with small negative curvatures, in agreement with semiempirical Born models and experimental data.[39–44]

Since the bulk modulus is nearly linear with pressure, the V/V_0 curves are roughly determined by B_0 and its first derivative at zero pressure, B_0'. B_0 is close to 30 GPa for LiCl and NaCl and around 15 GPa for KCl and RbCl (see Table I). B_0', as computed by Lagrange increments, is about 4 for these ACl crystals. Hence, we expect to find similar V/V_0-P curves for LiCl and NaCl and analogous although stiffer curves for KCl and RbCl. Some numbers confirm these conjectures: At $P = 10$ GPa, $V/V_0 \simeq 0.80$ for LiCl and NaCl and about 0.70 for KCl and RbCl; at 60 GPa, V/V_0 values are 0.53 (LiCl), 0.56 (NaCl), 0.44 (KCl), and 0.40 (RbCl) (not included in Fig. 2). The small differences in the high-pressure region are mainly due to differences in B_0' (see Table II).

The above analysis is also valid for B2 curves. According to Fig. 2, B-P slopes for B2 phases are very similar to those of B1 structures. The important conclusion we can draw from this reasoning, along with the previous discussed sign of $B_0(\text{B1}) - B_0(\text{B2})$, is the following: B1 and B2 V/V_0-P curves tend to be more separated as P increases for LiCl and NaCl crystals in a wide range of pressures; the opposite holds for KCl and RbCl. Considering now the product $P[V(B1) - V(B2)]/V_0$ as a driving pressure to start the B1-B2 transition phase[21] and bearing in mind that the difference $[V(B1) - V(B2)]/V_0$ at zero P increases with the cation size, our analysis would suggest low transition pressures for KCl and RbCl and high transition pressures for LiCl and NaCl. In fact, such behavior is found in our explicit calculations of transition pressures (see below) and in the experimental measurements.

The calculated static V/V_0-P curves show discrep-

ancies with respect to room-temperature experimental data. These differences are very small for B1 phases in the low-pressure region. For NaCl, where data for the B1 phase are available up to ~30 GPa, calculations tend to underestimate slightly the relative density. For B2 phases, the differences are bigger and opposite in sign, especially in the high-pressure regime, where static compression data are available up to 70 GPa for NaCl (Ref. 23) and to 56 GPa for KCl (Ref. 24). These discrepancies, we believe, are due in large part to thermal effects. We can displace either theoretical or experimental data to the same temperature scale using the well-known Mie-Grüneisen EOS. However, this procedure involves empirical information such as Debye temperatures and Grüneisen parameters of the ACl crystals. Instead, we have chosen here a different procedure. Recently, Thakur and Dwary[30] have shown that P-V data of the NaCl B1 phase at 298, 500, and 800 K can be reduced to a single curve by plotting $V(T)/V_0(T)$ versus $P/B_0(T)$. Assuming that this single curve holds for the ACl crystals in both structures, we have prepared analogous plots in Fig. 3 for LiCl (B1), NaCl (B1,B2), and KCl (B2) in the ranges of available experimental data. Values of B_0 at 298 K and zero pressure for the stable B1 phases are 31.85 GPa (LiCl),[42] 24 GPa (NaCl),[43] and 18.2 GPa (KCl).[10] For the unaccessible B2 structures we have used the B_0 values from Jeanloz's finite strain fitting[45] of the high-pressure measurements: 36.2 GPa (NaCl)[23] and 28.7 GPa (KCl).[24]

Some criticism should be made at this point: first, the use of extrapolated B_0 parameters in the last two cases and, second, and perhaps more important, the potential

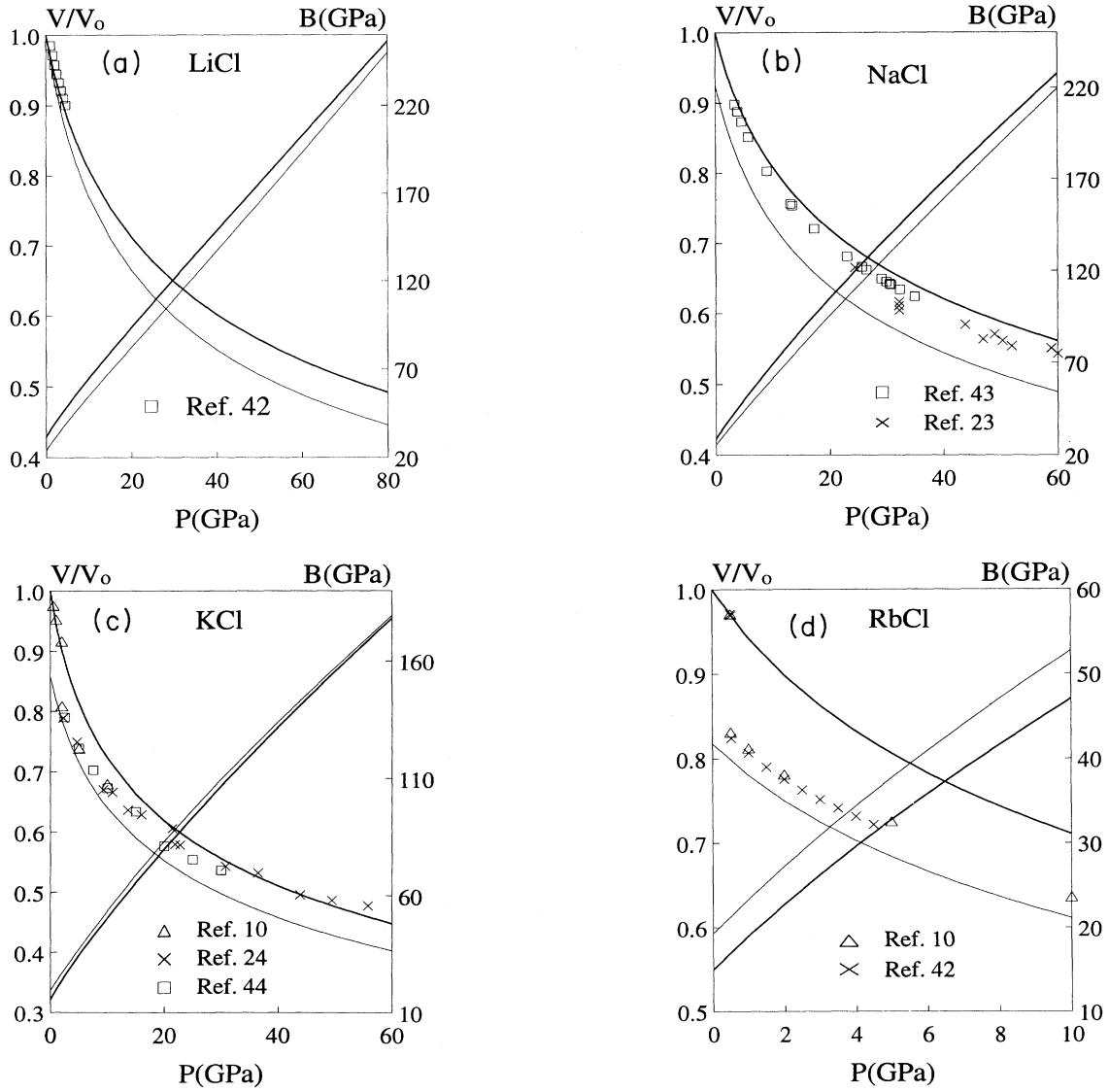

FIG. 2. Static V/V_0-P and B-P diagrams. Thick and thin curves stand for B1 and B2 structures. Symbols represent experimental data at 298 K. (a) LiCl, (b) NaCl, (c) KCl, and (d) RbCl.

cancellation of errors when managing ratios of magnitudes. Luckily or not, theoretical curves agree now with the experimental points for all the crystals and structures we have studied (see Fig. 3). It is worthwhile to remark on the results obtained in the extensively measured NaCl (B1,B2) and KCl (B2) crystals. According to Fig. 2, 0-K static predictions underestimate (overestimate) the B1 (B2) room-temperature crystal density of NaCl and KCl. These two opposite discrepancies are almost completely removed in the temperature-scaled diagrams of Fig. 3, showing that the agreement between theory and experiment is not so fortuitous.

We have carried out one more general test of the calculated EOS, involving not direct comparisons with experiments but consistency with the empirical behavior found in many real solids. We have chosen the *universal* EOS of Vinet *et al.*[31] (VEOS) as a measure of the degree of realism of our modeled solids. This form has been very recently tested in a wide variety of compounds, including the ACl crystals, showing better fittings than other phenomenological EOS.[38,46] VEOS connects isothermal P-V data through the equation

$$\ln H = \ln B_0 + \tfrac{3}{2}(B_0' - 1)(1 - x), \tag{3}$$

where H and x are defined as

$$H = \frac{Px^2}{3(1-x)}, \quad x = \frac{V}{V_0}. \tag{4}$$

We have fitted the VEOS to our computed P-V data. Graphical results are displayed in Fig. 4. The thick (thin) curves stand for the B1 (B2) structures, the small

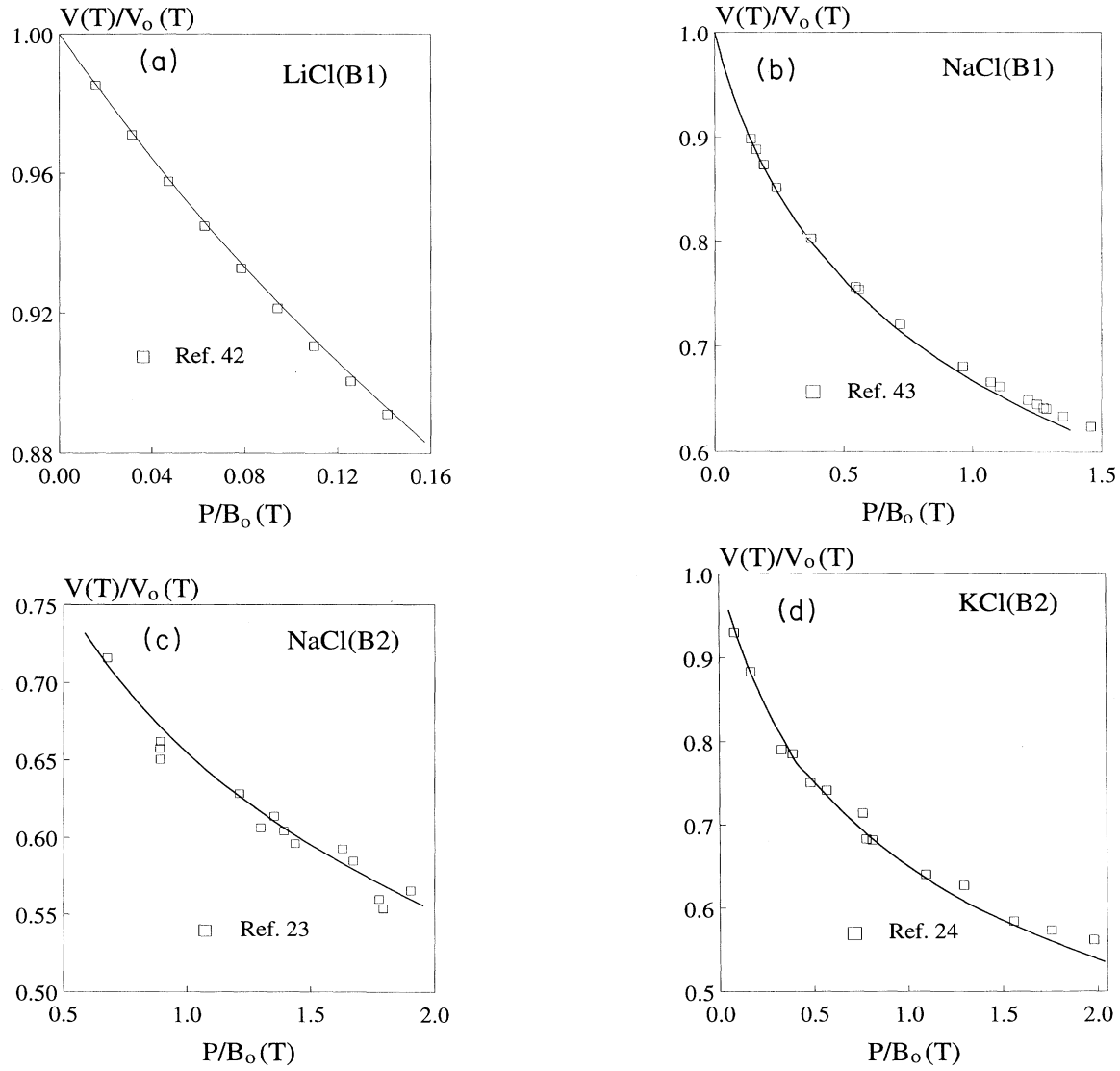

FIG. 3. Temperature-scaled diagrams. Curves stand for our static calculations. Symbols represent experimental data at 298 K. (a) LiCl(B1), (b) NaCl(B1), (c) NaCl(B2), and (d) KCl(B2).

black squares being the theoretical values. Table II collects elastic parameters (B_0, B_0') and regression coefficients from the fitting. Departures from 1.0 of our regression coefficients are around 0.001. This result is highly rewarding since the fluctuations found for regression coefficients from experimental EOS (Refs. 38 and 47) lie in analogous intervals.

As a consequence of the linearity of the plots in Fig. 4, B_0 values in Table II are very close to those calculated with the zero-T, $PE_{\rm latt}(a)$ curves (Table I). B_0' is in the range of 4.30±0.45 (except for CsCl), somewhat below the experimental values at room temperature (5.50±0.13) quoted by Shanker, Jain, and Singh.[48] However, it should be noted that measured values of B_0' are doubtlessly increasing functions of T.[49] Spetzler, Sammis, and O'Connell[36] have extrapolated high-temperature B_0' measurements to 0 K in NaCl (B1), predicting a value of 4.88, which is very close to our VEOS one (4.75). Besides the quantitative agreement, we want to emphasize that the *AIPI* descriptions behave as VEOS solids in the ranges of pressures analyzed. We believe that the success in this kind of test is an important requisite to verify the ability of QM solid-state methodologies in a reliable simulation of solid materials.

Going from the particular to the general behavior, a more valuable EOS is left. If it were possible, that would be a reduced equation for all the *A*Cl crystals. This kind of equation must resort to key variables upon which other properties depend. A key variable for ionic crystals is the equilibrium lattice parameter, which explains a number of trends of several magnitudes. In fact, we have already reduced some results by scaling volumes with V_0. From

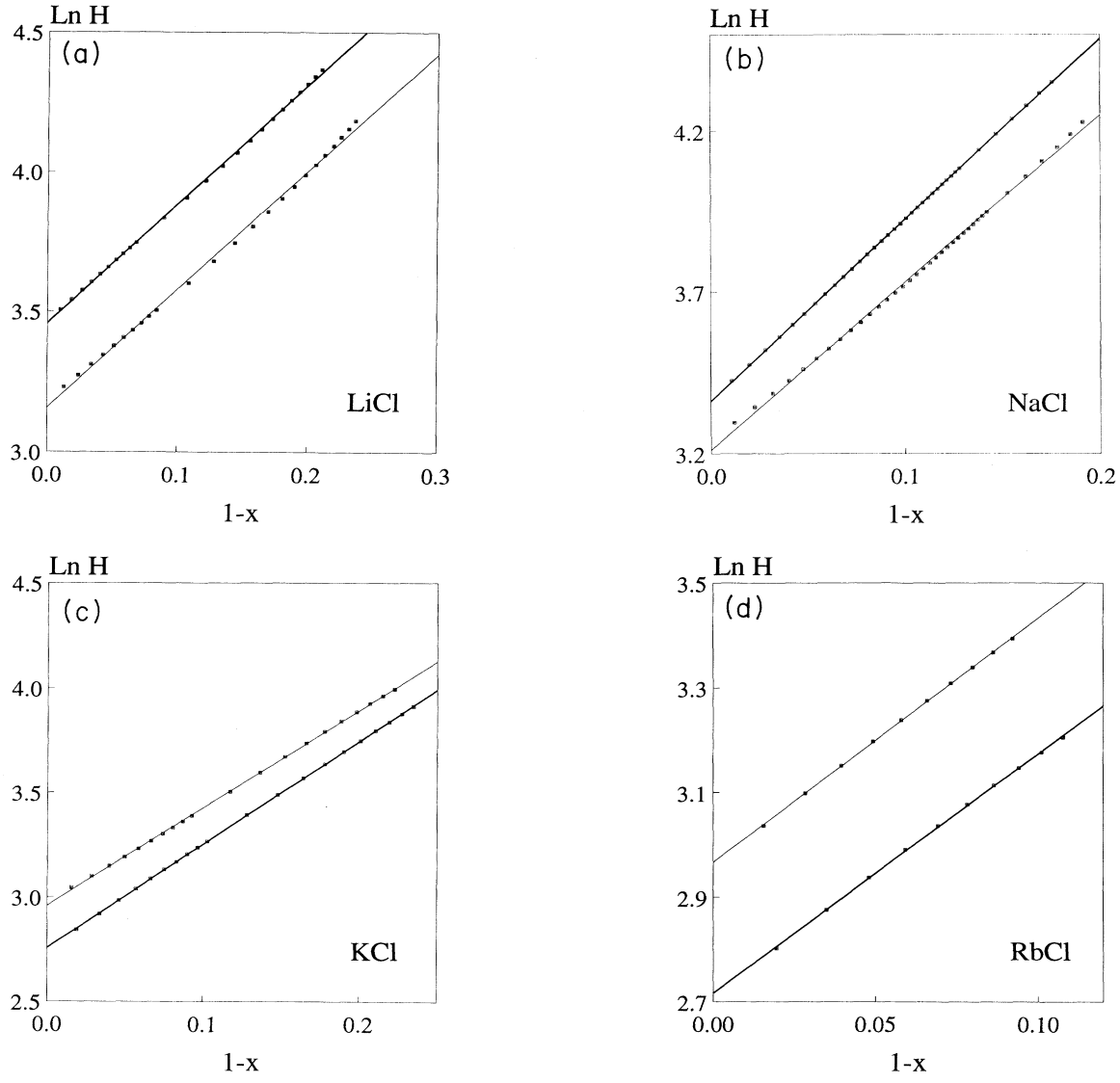

FIG. 4. VEOS. Symbols are calculated points. Thick and thin curves represent fitted VEOS for B1 and B2 structures. (a) LiCl, (b) NaCl, (c) KCl, and (d) RbCl.

TABLE II. Elastic parameters and regression coefficients (RC's) from VEOS fitting.

		LiCl	NaCl	KCl	RbCl	CsCl
B_0 (GPa)	B1	31.74	28.85	15.77	15.91	9.91
	B2	23.51	24.81	19.30	20.26	12.49
B_0'	B1	3.84	4.75	4.29	3.59	1.70
	B2	3.81	4.46	4.11	3.66	2.83
RC	B1	0.99977	0.99998	0.99998	0.99745	0.99986
	B2	0.99903	0.99923	0.99990	0.99765	0.99250

the analysis in this section, we have seen that the ACl EOS are rather determined by B. This suggests the use of the bulk modulus as a reduction parameter of P-V data. Among the different ways to relate reduced pressure with reduced volume, we have chosen one with some physical meaning. Following Flowers and Mendoza,[50] the quotient P/B can be expressed in term of a series:

$$\frac{P}{B} = -\sum_j a_j s^j, \tag{5}$$

where a_j are coefficients depending on the material, and the strain s is defined as

$$s = \frac{V - V_0}{V_0}. \tag{6}$$

If all the a_j coefficients were zero except $a_1 = 1$, the solid obeys Hooke's law and behaves harmonically. This is indeed the limiting case for zero P in any crystal. Real crystals show anharmonicity, and the number of nonzero a_j coefficients increases with P.

Therefore, we can also explore anharmonicity terms in the ACl crystals plotting $-s$ (strain) versus P/B (stress). Figure 5 contains the computed strain-stress values for LiCl, NaCl, KCl, and RbCl in B1 and B2 phases. For $-s$ less than 0.25, all the points seem to obey a unique Eq. (5), with a_j=0 for j >2. For $-s$ >0.25, points fall in a wider band, showing negative cubic terms for KCl and RbCl.

This plot gives some useful practical and theoretical information. In a range of a few GPa, ACl crystals behave harmonically. As pressure increases, anharmonicity develops with a similar strength for the four crystals up to ~15 GPa. It is within this pressure range where ACl crystals can be described with a single reduced EOS. Above this pressure, departure from Hooke's law changes with the cation size. This behavior may be related to the crystal hardness, which we define as the rate at which E_{latt} goes to infinite as a goes to zero from the equilibrium position. Since this rate is lower for the harmonic limit, the strain-stress curves should stand above the Hooke's line,[50] as is the case in Fig. 5. From this figure, it is shown that crystal hardness is a function of the compound, the phase, and the pressure. Dependence on these variables is not easy to describe.

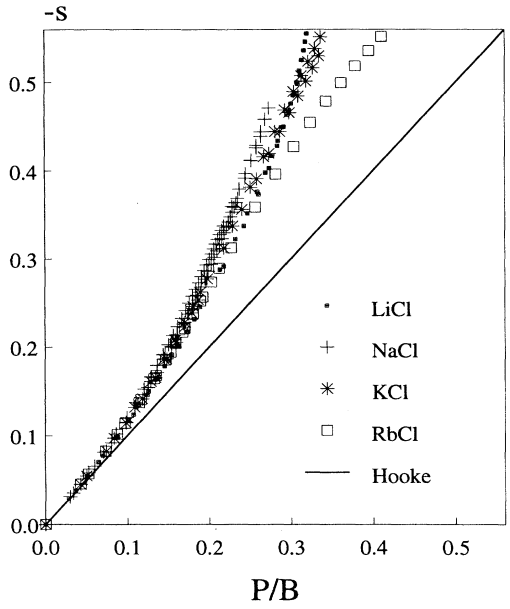

FIG. 5. Strain-stress diagram.

C. Phase transitions

We have analyzed crystal-phase stability using the following equation:

$$\Delta G(P) = \Delta E_{\text{latt}}(P) + P\Delta V(P), \tag{7}$$

where Δ means differences between magnitudes in B1 and B2 phases. The thermodynamic 0-K transition pressure P_t is defined as the P value that makes $\Delta G = 0$. Pressures with negative (positive) ΔG values show regions with B1 (B2) stability. The evolution of the computed $\Delta G(P)$ function is plotted in Fig. 6 for the five ACl

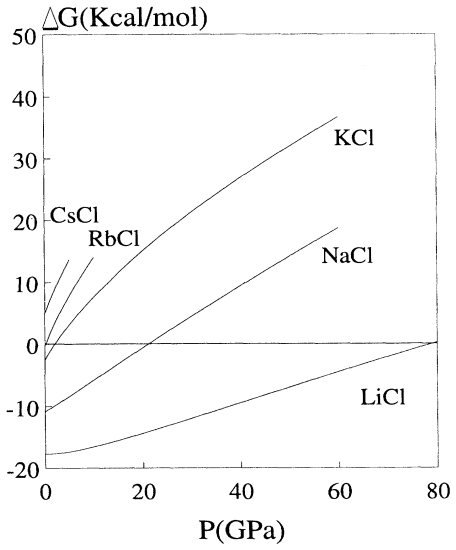

FIG. 6. P dependence of ΔG.

crystals. These curves show a high regularity in passing from LiCl to CsCl: (a) ΔG values at zero P increase with the cation size, being negative for LiCl, NaCl, KCl, and RbCl and positive for CsCl, in agreement with the experiments; (b) P_t decreases with the cation size, as the available experimental data do; (c) the slope of ΔG computed at P_t (which is nothing but the transition volume, ΔV_t) increases with the cation size, in agreement again with the observed trend.

Theoretical predictions of several B1-B2 transition magnitudes are collected in Table III along with room-temperature available experimental data. The computed P_t values tend to underestimate the range of B1 stability. Our result for NaCl (22 GPa) is very close to the value obtained in careful LDA calculations by Feldman, Mehl, and Krakauer[20] (21.4 GPa). P_t is a very sensitive magnitude depending strongly on computational parameters. Thus, according to our calculations, a biased change of 1 kcal/mol in $\Delta E_{\rm latt}$ at zero P would modify the prediction of P_t by about 4, 2, 1, and 0.5 GPa in LiCl, NaCl, KCl, and RbCl, respectively. Slight variations of $P\Delta V$ also modify P_t. From Table III, we see that the computed values of $-\Delta V_t/V_t$(B1) are somewhat larger than the room-temperature experimental values. Therefore, it is very likely that an overestimation of the computed $P\Delta V$ term causes low-transition-pressure predictions for these crystals.

Unfortunately, there are no direct measurements of ΔB_t. Heinz and Jeanloz[23] have estimated a reduction of B in NaCl by about -6%, and they quote the prediction of Jeanloz to be between -8% and -12%. From Yagi's data on KCl,[51] we estimate a ΔB_t of 7%. A higher value (14%) can be estimated from Campbell-Heinz EOS of KCl.[24] These trends agree with the corresponding computed values and the different sign of $\Delta B_t/B_t$(B1) we have found for NaCl (-9%) and KCl (13%).

TABLE III. Transition-phase data of alkali chlorides. First row: theoretical calculations. Second row: experimental data at 298 K.

		LiCl	NaCl	KCl	RbCl
P_t (GPa)	Calc.	~80	22	2	0.2
	Expt.		26.8[a] -30[b]	2[c]	0.5[c]
V_t(B1) (cm^3/mol)	Calc.	10.3	18.6	37.9	45.6
	Expt.		17.36[b]	34.35[c]	41.43[c]
V_t(B2) (cm^3/mol)	Calc.	9.3	16.5	33.0	37.5
	Expt.		16.37[b]	30.14[c]	35.38[c]
$-\Delta V_t/V_t$(B1)	Calc.	0.09	0.11	0.13	0.18
	Expt.		0.058[b]	0.122[c]	0.146[c]
B_t(B1) (GPa)	Calc.	256	111	24	17
	Expt.				
B_t(B2) (GPa)	Calc.	250	102	27	21
	Expt.				
$-\Delta B_t/B_t$(B1)	Calc.	-0.03	-0.09	0.13	0.26
	Expt.				

[a]Ref. 21.
[b]Ref. 22.
[c]Ref. 42.

In spite of the fact that only fair agreement between theoretical and experimental transition data is achieved at the quantitative level, we want to remark that the overall view is satisfactory. Transition properties change from LiCl to CsCl in the correct direction, providing valuable support for phenomenological and empirical models. We will show that kind of connection with other models in the following discussions.

An alternative estimation of P_t can be obtained by

$$P_t \simeq -\frac{\Delta E_{\rm latt}(P)}{\Delta V(P)}, \tag{8}$$

which is exact at $P = P_t$. Our computed P_t values from Eq. (8) show that this is a good approximation for the ACl crystals in a wide range of pressures before P_t is reached. This is due to the P-independent behavior shown by $\Delta E_{\rm latt}$ and the rather constant evolution of ΔV with P after a quick increase in the low-pressure range.

Majewski and Vogl[52] have recently called attention to the fact that the B1-B2 transition pressures of ionic crystals strongly depend on the cation but only weakly on the anion. These authors analyzed the phenomenon in terms of a simple universal tight-binding model. They suggested that P_t is mainly determined by the quotient $-\Delta E_{\rm latt}/\Delta V$ evaluated at zero pressure. We can check this suggestion with our data. The transition pressures given by $-\Delta E_{\rm latt}(0)/\Delta V(0)$ are 22.3 GPa (NaCl), 1.8 GPa (KCl), and 0.16 GPa (RbCl), in remarkable agreement with the P_t values obtained by solving $\Delta G(P)=0$ (see Table III). For LiCl, however, the relation used by Majewski and Vogl incorrectly predicts a negative transition pressure, as our computed $\Delta V(0)$ and $\Delta E_{\rm latt}(0)$ are negative numbers. Taking this case as a warning, we can conclude that $\Delta E_{\rm latt}(P = 0)$ and $\Delta V(P = 0)$ roughly determine P_t, as suggested by Majewski and Vogl. As $\Delta E_{\rm latt}(P = 0)$ decreases and $\Delta V(P = 0)$ increases with the cation size (see Table I), our calculations predict correctly the strong cation dependence of P_t.

To end this section, we extract from our computations some additional information concerning the transition phase process in the ACl crystals. In Fig. 7, we plot again the computed V/V_0-P curves for the B1 and B2 phases of NaCl. In this case, we have limited the pressure range to 15–30 GPa. Arrows show the hysteresis cycle of the transition. The width of the metastability region (6.9 GPa) is taken from the room-temperature data of Li and Jeanloz.[21] Since our computed P_t value is 22 GPa for NaCl, P values confining that region are 18.55 GPa ($P_{\rm B2\text{-}B1}$) and 25.45 GPa ($P_{\rm B1\text{-}B2}$). The existence of B1 or B2 in this interval of pressures depends on the history of the sample (thick lines). The solid and thin lines below $P_{\rm B2\text{-}B1}$ and above $P_{\rm B1\text{-}B2}$ show regions with stable B1 and B2 phases, respectively. Finally, dashed lines describe situations with unstable crystalline phases.

According to the Li-Jeanloz analysis of the observed

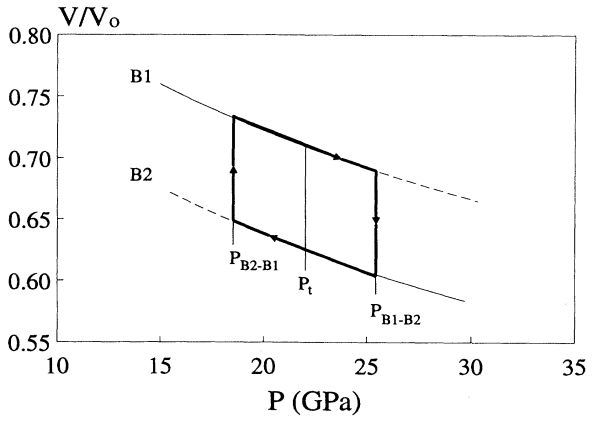

FIG. 7. Hysteresis cicle for NaCl B1-B2 phase transition.

coexistence boundaries of B1 and B2 phases in NaCl,[21] the magnitude of $\Delta G(P)$ plays a decisive role in the phase transformation. These authors approximate the thermodynamic driving force corresponding to the overpressure or underpressure $\Delta G(P)$ by the following equation:

$$\Delta G(P) = \Delta V_t(P - P_t). \tag{9}$$

To see how good this approximation is, we can add a null value $-\Delta G(P_t)$ to the right side of Eq. (7):

$$\Delta G(P) = \Delta E_{\text{latt}}(P) - \Delta E_{\text{latt}}(P_t) + P\Delta V(P) - P_t\Delta V(P_t), \tag{10}$$

which reduces to Eq. (9) if both ΔE_{latt} and ΔV behave as constants. We have discussed earlier that these magnitudes do not change appreciably with P. Therefore, our calculations reinforce some of the assumptions of the Li-Jeanloz model.[21]

For NaCl, the predicted limits for the thermodynamic driving force are 1.62 kcal/mol (overpressure) and 1.57 kcal/mol (underpressure). The closeness of these values could be connected with the symmetry of the coexistence curves proposed by Li and Jeanloz, which suggest the use of the average of $P_{\text{B1-B2}}$ and $P_{\text{B2-B1}}$ to locate the thermodynamic transition pressure P_t (see Fig. 7).

It should be noted finally that the overpressure (underpressure) needed to reach those limit values of thermodynamic driving forces changes strongly with the cation size. This becomes evident when analyzing $\Delta G(P)$ curves in Fig. 6, which may be roughly described by straight lines with slopes 0.1 (LiCl), 0.5 (NaCl), 1 (KCl), and 2 (RbCl) in kcal mol^{-1}/GPa units. In the context of the combined thermodynamic-kinetic model of Li and Jeanloz,[21] these results suggest a decreasing interval of the metastability region in passing from LiCl to RbCl, which is in agreement with the available experimental data reported so far.[21,53,54]

IV. CONCLUSIONS

A well-tested quantum-mechanical methodology, the *AIPI* model, has been applied to study the crystal response to pressure in the B1 and B2 phases of the alkali chloride family. The results have been used to determine zero-T, P cohesive properties, several zero-T static EOS, and B1-B2 transition data. The whole analysis has been performed from a macroscopic-thermodynamic point of view.

For the equilibrium lattice parameters and lattice energies, our predictions show discrepancies less than 5% with the experimental data. The stable zero-P crystal phases are correctly reported and changes in geometrical, energetic, and elastic properties in passing from LiCl to CsCl are found to follow the observed trends. Analogous behavior has been obtained for the properties explored in the unstable crystalline phases.

We have found that the *A*Cl EOS is mainly controlled by the zero-pressure bulk modulus and its first derivative. Our computed zero-temperature $V/V_0 - P$ curves deviate from the corresponding room-temperature experimental points as P increases. In principle, these deviations may be due to thermal effects since in the $V(T)/V_0(T) - P/B_0(T)$ temperature-scaled diagram the experimental data straddle the theoretical curve over the whole computed range of pressures. It should be emphasized here that static zero-T EOS and room-temperature P-V data have been displaced to the same scale without resorting to any empirical parameter.

A major test of the computed EOS has been the *universal* VEOS fitting. We found that the *AIPI* results do fit the VEOS as do the real solids and propose this kind of test to check the reliability of the QM methodologies. From the strain-stress plot, we have illustrated that (a) it is possible to describe the *A*Cl family with a single EOS in the 0–15-GPa region, and (b) the departure from Hooke's behavior is a complicated function of the compound, the phase, and the pressure.

Finally, we have obtained thermodynamic transition pressures that tend to underestimate the observed stability region for the B1 phase. For the not-yet measured LiCl B1-B2 transition, our computed value is close to 80 GPa. The predicted transition properties mimic well the available experimental data. Moreover, our work supports several ideas deduced from semiempirical models proposed to understand the complexity of the B1-B2 transition phase. Our computations found a basis for further investigation at the microscopic-quantum level which is currently in progress.[25]

ACKNOWLEDGMENTS

We want to express our gratitude to Professor L. Pueyo for clarifying suggestions and the careful reading of the manuscript. We are grateful to the Centro de Cálculo Científico, Universidad de Oviedo, for the CONVEX facility in which the calculations have been done. Financial support from the Spanish Dirección General de Investigación Científica y Tecnológica (DGICYT), Project No. PB90-0795, is also acknowledged.

[1] S. Eliezer, in *High-Pressure Equations of State: Theory and Applications*, edited by S. Eliezer and R. A. Ricci (North-Holland, Amsterdam, 1991), p. 1, and references therein.
[2] M. Born and K. Huang, *Dynamical Theory of Crystal Lattices* (Oxford University Press, New York, 1954).
[3] M. P. Tosi, Solid State Phys. **16**, 1 (1964).
[4] F. A. Khwaja, S. H. Naqvi, and M. S. K. Razmi, Phys. Status Solid B **143**, 453 (1987); F. A. Khwaja, M. S. K. Razmi, and S. H. Naqvi, *ibid.* **156**, 111 (1989).
[5] K. N. Jog, R. K. Singh, and S. P. Sanyal, Phys. Rev. B **31**, 6047 (1985).
[6] N. V. K. Prabhakar, R. K. Singh, N. K. Gaur, and N. N. Sharma, J. Phys. Condens. Matter **2**, 3345 (1990).
[7] B. S. Rao and S. P. Sanyal, Phys. Rev. B **42**, 1810 (1990).
[8] R. Gordon and Y. S. Kim, J. Chem. Phys. **56**, 3122 (1972).
[9] L. L. Boyer, M. J. Mehl, J. L. Feldman, J. R. Hardy, J. W. Flocken, and C. Y. Fong, Phys. Rev. Lett. **54**, 1940 (1985).
[10] L. Boyer, Phys. Rev. B **23**, 3673 (1981).
[11] J. L. Feldman, M. J. Mehl, L. L. Boyer, and N. C. Chen, Phys. Rev. B **37**, 4784 (1988).
[12] D. L. Decker, J. Appl. Phys. **42**, 3239 (1971).
[13] H. Zhang and M. S. T. Bukowinski, Phys. Rev. B **44**, 2495 (1991).
[14] P. O. Löwdin, Adv. Phys. **5**, 1 (1956).
[15] A. B. Kunz, Phys. Rev. B **26**, 2056 (1982).
[16] V. Luaña and L. Pueyo, Phys. Rev. B **41**, 3800 (1990).
[17] J. Yamashita and S. Asano, J. Phys. Soc. Jpn. **52**, 3506 (1983).
[18] W. Kohn and L. J. Sham, Phys. Rev. **140**, 1133 (1965).
[19] (a) S. Froyen and M. L. Cohen, Phys. Rev. B **29**, 3770 (1984); (b) J. Phys. C **19**, 2623 (1986).
[20] J. L. Feldman, M. J. Mehl, and H. Krakauer, Phys. Rev. B **35**, 6395 (1987).
[21] X. Li and R. Jeanloz, Phys. Rev. B **36**, 474 (1987).
[22] W. A. Basset, J. Takahashi, M. K. Mao, and J. S. Weaver, J. Appl. Phys. **39**, 319 (1968).
[23] D. L. Heinz and R. Jeanloz, Phys. Rev. B **30**, 6045 (1984).
[24] A. J. Campbell and D. L. Heinz, J. Phys. Chem. Solids **52**, 495 (1991).
[25] A. Martín Pendás, L. Kantorovich, E. Francisco, M. Flórez, J. M. Recio, and V. Luaña (unpublished).
[26] S. Huzinaga and A. A. Cantu, J. Chem. Phys. **55**, 5543 (1971); S. Huzinaga, D. McWilliams, and A. A. Cantu, Adv. Quantum Chem. **7**, 187 (1973).
[27] L. Pueyo, V. Luaña, M. Flórez, and E. Francisco, in *Structure, Interactions and Reactivity*, edited by S. Fraga (Elsevier, Amsterdam, 1992), Vol. B, p. 504.
[28] V. Luaña, M. Flórez, E. Francisco, A. Martín Pendás, J. M. Recio, M. Bermejo, and L. Pueyo, in *Cluster Models for Surface and Bulk Phenomena*, edited by G. Pacchioni, P. S. Bagus, and F. Parmigiani, Vol. 283 of *NATO Advanced Study Institute, Series B: Physics* (Plenum, New York, 1992), p. 605.
[29] J. M. Recio, R. Pandey, and V. Luaña, Phys. Rev. B **47**, 3401 (1993).
[30] K. P. Thakur and B. D. Dwary, J. Phys. C **19**, 3069 (1986).
[31] P. Vinet, J. Ferrante, J. R. Smith, and J. H. Rose, J. Phys. C **19**, L467 (1986).
[32] E. Clementi, IBM J. Res. Dev. **9**, 2 (1965); S. J. Chakravorty and E. Clementi, Phys. Rev. A **39**, 2290 (1989).
[33] E. Clementi and C. Roetti, At. Data. Nucl. Data Tables **14** (1974).
[34] E. R. Cowley, Z. Gong, and G. K. Horton, Phys. Rev. B **41**, 2150 (1990).
[35] A. J. Cohen and R. G. Gordon, Phys. Rev. B **12**, 3228 (1975).
[36] H. Spetzler, C. G. Sammis, and R. J. O'Connell, J. Phys. Chem. Solids **41**, 199 (1972).
[37] C. S. Smith and L. S. Cain, J. Phys. Chem. Solids **41**, 199 (1980).
[38] C. Li-Rong and C. Qing-Hu, J. Phys. Condens. Matter **3**, 775 (1991).
[39] P. B. Ghate, Phys. Rev. **139**, 1666 (1965).
[40] *Handbook of Chemistry and Physics*, 60th ed., edited by R. C. Weast (Chemical Rubber Co., Boca Raton, 1979).
[41] (a) C. Kittel, *Introduction to Solid State Physics*, 4th ed. (Wiley, New York, 1971); (b) *Introduction to Solid State Physics*, 2nd ed. (Wiley, New York, 1957).
[42] S. N. Vaidya and G. C. Kennedy, J. Phys. Chem. Solids **32**, 951 (1971).
[43] L. Liu and W. A. Basset, J. Appl. Phys. **44**, 1475 (1973).
[44] H. G. Drickamer, R. W. Lynch, R. L. Clendesen, and E. A. Pérez-Albuerne, Solid State Phys. **19**, 135 (1966).
[45] R. Jeanloz, Geophys. Res. Lett. **8**, 1219 (1981).
[46] S. K. Sikka, Phys. Lett. A **135**, 129 (1989).
[47] P. Vinet, J. H. Rose, J. Ferrante, and J. R. Smith, J. Phys. Condens. Matter **1**, 1941 (1989).
[48] S. Shanker, V. C. Jain, and J. P. Singh, Phys. Rev. B **22**, 1083 (1980).
[49] F. Birch, J. Geophys. Res. **91**, 4949 (1986).
[50] B. H. Flowers and E. Mendoza, *Properties of Matter* (Wiley, Chichester, 1990), p. 51.
[51] T. Yagi, J. Phys. Chem. Solids **39**, 563 (1978).
[52] J. A. Majewski and P. Vogl, Phys. Rev. Lett. **57**, 1366 (1986).
[53] N. Nakagiri and M. Nomura, J. Phys. Soc. Jpn. **51**, 2412 (1982).
[54] A. Lacam and J. Peyronneau, J. Phys. (Paris) **34**, 1047 (1973).